Molecular Weight Control of Polyethylene Waxes using a Constrained Imino-Cyclopenta[*b*]pyridyl-Nickel Catalyst

Zheng Wang,[a,b] Youfu Zhang,[b,c] Yanping Ma,[a] Xinquan Hu,*[,c] Gregory A. Solan,*[,b,d,] Yang Sun,[a] and Wen-Hua Sun*[,a,b]

(Zheng Wang and Youfu Zhang made an equal contribution in this work.)

[a] Key Laboratory of Engineering Plastics and Beijing National Laboratory for Molecular Science, Institute of Chemistry, Chinese Academy of Sciences, Beijing 100190, China.

[b] CAS Research/Education Center for Excellence in Molecular Sciences, University of Chinese Academy of Sciences, Beijing 100049, China.

[c] College of Chemical Engineering, Zhejiang University of Technology, Hangzhou 310014, China.

[d] Department of Chemistry, University of Leicester, University Road, Leicester LE1 7RH, UK.

Correspondence to: W.-H. Sun (E-mail: *whsun@iccas.ac.cn; xinquan@zjut.edu.cn; gas8@le.ac.uk*)

ABSTRACT: Five examples of nickel(II) bromide complexes bearing *N,N*-imino-cyclopenta[*b*]pyridines, [7-(ArN)-6-$Me_2C_8H_5N$]$NiBr_2$ (Ar = 2,6-$Me_2C_6H_3$ (**Ni1**), 2,6-$Et_2C_6H_3$ (**Ni2**), 2,6-*i*-$Pr_2C_6H_3$ (**Ni3**), 2,4,6-$Me_3C_6H_2$ (**Ni4**), 2,6-Et_2-4-MeC_6H_2 (**Ni5**)), have been prepared by the reaction of the corresponding ligand, **L1 – L5**, with $NiBr_2$(DME) (DME = 1,2-dimethoxyethane). On crystallization from bench dichloromethane, **Ni1** underwent adventitious reaction with water to give the aqua salt, [**L1**$NiBr(OH_2)_3$][Br] (**Ni1'**). The molecular structures of **Ni1'** and **Ni3** have been structurally characterized, the latter revealing a bromide-bridged dimer. On activation with either MMAO or Et_2AlCl, **Ni1**, **Ni2**, **Ni4** and **Ni5**, all exhibited high activities for ethylene polymerization (up to 3.88 × 10^6 g(PE)·mol^{-1}(Ni)·h^{-1}); the most sterically bulky **Ni3** gave only low activity. Polyethylene waxes are a feature of the materials obtained which typically display low molecular weights, narrow molecular weight distributions and unsaturated vinyl and vinylene functionalities. Notably, the catalyst comprising **Ni1**/Et_2AlCl produced polyethylene with the lowest molecular weight, 0.67 Kg·mol^{-1}, which is less than any previously reported data for any class of cycloalkyl-fused pyridine-nickel catalyst.

KEYWORDS: N,N-imino-cyclopenta[b]pyridines; Polyethylene; coordination/insertion polymerization; nickel complex.

INTRODUCTION

Since the first report of α-diimino-nickel pre-catalysts in ethylene polymerization in the mid-1990's,[1] the intervening years have seen numerous developments in catalyst design that have impacted on a wide range of properties such as catalyst activity, molecular weight of the polyethylene through to the distribution of oligomer/polymer.[2] In addition, the degree of branching within the polymer can be influenced by the choice of nickel catalyst to the point that the resultant materials can sometimes show properties reminiscent of linear low density polyethylene.[2,3] Central to these performance and structural variations is the nature of the

ancillary ligand with bidentate, N^N,[4] N^O[5] and N^P[6] as well as tridentate ligands, N^N^N,[7] N^P^N,[8] O^N^N[9] and P^N^P[10] commonly employed.

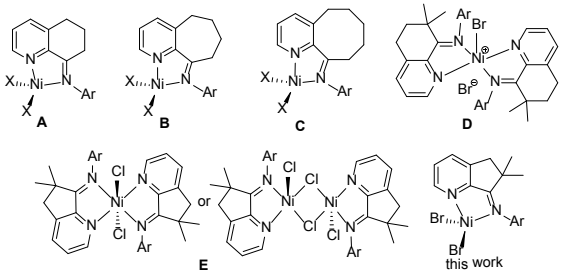

Chart 1. Previous and to be developed cycloalkyl-fused pyridyl-nickel pre-catalysts (**A** - **E**)

Recent years have seen the introduction of cycloalkyl-fused pyridines as compatible N,N-ligand frames for nickel with some examples including the cyclohexyl-, cycloheptyl- and cyclooctyl-derivatives **A**,[11] **B**[12] and **C**, respectively (Chart 1).[13] Indeed **A** - **C** exhibit high activities in ethylene polymerization generating polyethylenes of generally low molecular weight but with their specific range depending on the ring size.[11a,11b,12,13] To address issues associated with undesirable imine-enamine tautomerization processes that have affected some of these cycloalkyl-fused systems,[14] the *gem*-dimethyl cyclohexyl-containing **D**[15] (Chart 1) has been subsequently disclosed.[16] While the activity of **D** is lower when compared to its closest comparator **A**, it displays slightly lower molecular weight and a narrower molecular weight distribution for the polymer. Subsequently, the more strained 6,6-dimethyl-iminocyclopenta[*b*]pyridyl-nickel chlorides (**E**, Chart 1)[16] have been developed that generate polyethylenes with even lower molecular weight, narrower polydispersities and contain vinyl and vinylene groups. To the best of our knowledge, **E** is the first of its kind to promote the formation of vinyl- and vinylene-polyethylenes by an ethylene homo-polymerization process. With regard to steric effects,[17] all the cycloalkyl-fused pyridine systems, **A** – **E**, give enhanced catalytic performance with less sterically hindered N-aryl groups. On the other hand electronic factors can show some notable differences. For example, electron donating groups at the *para*-position of the N-aryl group enhance catalytic performance for **B** and **C** while for **A** and **E** the opposite trend is observed.[11a,12a,13]

Given the unusual properties of the polymer exhibited with **E** as the pre-catalyst and the sensitivity of cycloalkyl-pyridine ligand frame to steric and electronic variations, we decided to re-examine the polymerization using a slightly modified pre-catalyst. In particular, we explore in this work the catalytic performance of the 1:1 6,6-dimethyl-7-aryliminocyclopenta[*b*]pyridyl-nickel bromides (Chart 1) in ethylene polymerization. Notably, in previous work we have noted that the nature of the halide ligand in the pre-catalyst can influence to some degree both the activity and molecular weight.[11-13] A detailed catalytic evaluation will be reported while full synthetic and characterization data will be disclosed.

EXPERIMENTAL

General Considerations. All manipulations involving air- and/or moisture-sensitive compounds were performed under an atmosphere of nitrogen using standard Schlenk techniques. Prior to use, toluene was refluxed over sodium-benzophenone and distilled under an atmosphere of nitrogen. Methylaluminoxane (MAO, 1.46 M in toluene) and modified methylaluminoxane (MMAO, 1.93 M in *n*-heptane) were purchased from Akzo Nobel Corp. Diethylaluminum chloride (Et_2AlCl, 1.17 M in toluene) and ethylaluminum sesquichloride (EASC, 0.87 M in *n*-hexane) were purchased from Acros Chemicals. High-purity ethylene was purchased from Beijing Yanshan Petrochemical Co. and used as received. Other reagents were purchased from Aldrich, Acros or local suppliers. IR spectra were recorded on a Perkin-Elmer System 2000 FT-IR spectrometer. Elemental analysis was carried out using a Flash EA 1112 microanalyzer. Molecular weights (M_w) and molecular weight distributions (M_w/M_n) of the polyethylenes were determined using a PL-GPC220 instrument at 150 °C with 1,2,4-

trichlorobenzene as the solvent. The melting temperatures (T_m) of the polyethylenes were measured from the second scanning run on a PerkinElmer TA-Q2000 differential scanning calorimeter (DSC) under a nitrogen atmosphere. In the procedure, a sample of about 5.0 mg was heated to 140 °C at a rate of 20 °C/min and kept for 2 min at 140 °C to remove the thermal history and then cooled at a rate of 20 °C/min to -40 °C. ^{1}H NMR, ^{13}C NMR and DEPT135 ^{13}C NMR spectra of the polyethylenes were recorded on a Bruker DMX 300 MHz instrument at 100 °C in deuterated 1,1,2,2-tetrachloroethane with TMS as an internal standard. The imino-cyclopenta[*b*]pyridines, 7-(ArN)-6-$Me_2C_8H_5N$ (Ar = 2,6-$Me_2C_6H_3$ (**L1**), 2,6-$Et_2C_6H_3$ (**L2**), 2,6-*i*-$Pr_2C_6H_3$ (**L3**), 2,4,6-$Me_3C_6H_2$ (**L4**), 2,6-Et_2-4-MeC_6H_2 (**L5**)), were prepared using previously reported procedures.[16]

Synthesis of nickel complexes

[7-{(2,6-$Me_2C_6H_3$)N}-6-$Me_2C_8H_5N$]$NiBr_2$ (Ni1). $NiBr_2$(DME) (0.083 g, 0.27 mmol) was added to a solution of **L1** (0.079 g, 0.30 mmol) in CH_2Cl_2 (10 mL). The mixture was stirred for 12 h and then diethyl ether poured into the mixture to precipitate the complex. The precipitate was collected by filtration, washed with diethyl ether and dried under reduced pressure at 50 °C for 3 h to give **Ni1** as a red powder (0.120 g, 93%). FT–IR (KBr, cm^{-1}): 2979 (w), 2918 (w), 2873 (w), 1631 ($\nu_{C=N}$, s), 1608 (s), 1456 (s), 1432 (m), 1378 (w), 1298 (m), 1174 (s), 1022 (w), 879 (w), 795 (vs). Anal. Calcd for $C_{18}H_{20}Br_2N_2Ni$: C, 44.77; H, 4.17; N, 5.80. Found: C, 44.32; H, 4.30; N, 5.68.

[7-{(2,6-$Et_2C_6H_3$)N}-6-$Me_2C_8H_5N$]$NiBr_2$ (Ni2). Using a procedure similar to that described for **Ni1** but with **L2** in place of **L1**, **Ni2** was isolated as an orange powder (0.122 g, 89%). FT–IR (KBr, cm^{-1}): 2973 (w), 2930 (w), 2876 (w), 1634 ($\nu_{C=N}$, s), 1610 (s), 1451 (s), 1432 (m), 1331 (m), 1296 (m), 1169 (s), 1023 (w), 881 (w), 798 (vs). Anal. Calcd for $C_{20}H_{24}Br_2N_2Ni$: C, 47.02; H, 4.73; N, 5.48. Found: C, 47.13; H, 4.92; N, 5.25.

[7-{(2,6-*i*-$Pr_2C_6H_3$)N}-6-$Me_2C_8H_5N$]$NiBr_2$ (Ni3). Using a procedure similar to that described for **Ni1** but with **L3** in place of **L1**, **Ni3** was isolated as a red powder (0.127 g, 88%). FT–IR (KBr, cm^{-1}): 2961 (m), 2935 (w), 2864 (w), 1631 ($\nu_{C=N}$, s), 1606 (s), 1454 (s), 1439 (m), 1362 (w), 1298 (m), 1170 (s), 1023 (w), 879 (w), 803 (s). Anal. Calcd for $C_{22}H_{28}Br_2N_2Ni$: C, 49.03; H, 5.24; N, 5.20. Found: C, 48.77; H, 4.92; N, 5.40.

[7-{(2,4,6-$Me_3C_6H_2$)N}-6-$Me_2C_8H_5N$]$NiBr_2$ (Ni4). Using a procedure similar to that described for **Ni1** but with **L4** in place of **L1**, **Ni4** was isolated as a red powder (0.124 g, 93%). FT–IR (KBr, cm^{-1}): 2960 (w), 2923 (w), 2866 (w), 1635 ($\nu_{C=N}$, s), 1617 (s), 1455 (m), 1429 (w), 1378 (w), 1214 (w), 1187 (w), 1022 (m), 888 (m), 802 (s). Anal. Calcd for $C_{19}H_{22}Br_2N_2Ni$: C, 45.93; H, 4.46; N, 5.64. Found: C, 45.43; H, 4.87; N, 5.44.

[7-{(2,6-Et_2-4-MeC_6H_2)N}-6-$Me_2C_8H_5N$]$NiBr_2$ (Ni5). Using a procedure similar to that described for **Ni1** but with **L5** in place of **L1**, **Ni5** was isolated as an orange powder (0.135 g, 95%). FT–IR (KBr, cm^{-1}): 2971 (w), 2927 (w), 2873 (w), 1636 ($\nu_{C=N}$, s), 1609 (m), 1457 (s), 1433 (w), 1334 (m), 1296 (w), 1165 (w), 1022 (w), 881 (w), 858 (m), 797 (s). Anal. Calcd for $C_{21}H_{26}Br_2N_2Ni$: C, 48.05; H, 4.99; N, 5.34. Found: C, 48.44; H, 4.79; N, 5.57.

Ethylene polymerization at 5/10 atm ethylene pressure. The polymerization at high ethylene pressure was carried out in a stainless steel autoclave (250 mL capacity) equipped with an ethylene pressure control system, a mechanical stirrer and a temperature controller. The autoclave atmosphere was evacuated and the autoclave was filled with ethylene three times. When the desired reaction temperature was reached, 30 mL of toluene (freshly distilled) was added under ethylene atmosphere and the solution of the nickel pre-catalyst **(Ni1 – Ni5)** in another toluene (50 mL) was injected. The required amount of co-catalyst (MAO, MMAO, $EtAlCl_2$, EASC) and additional toluene (20 mL) were added by syringe successively. Then the ethylene pressure was increased to the desired value and the stirring initiated. After the required reaction time, the reactor was cooled

with an ice-water bath and the excess ethylene was vented. The resultant mixture was poured into 10% solution of HCl in ethanol, and the polymer was collected and washed with ethanol several times and dried in vacuo to constant weight.

X-ray crystallographic study

Single crystals of **Ni1'** and **Ni3** suitable for X-ray diffraction were obtained by slow diffusion of diethyl ether into a dichloromethane solution of the corresponding complex at room temperature. X-ray studies were carried out on a Rigaku Saturn724 + CCD with graphite-monochromatic Mo-Kα radiation (λ = 0.71073 Å) at 173(2) K; cell parameters were obtained by global refinement of the positions of all collected reflections. Intensities were corrected for Lorentz and polarization effects and empirical absorption. The structures were solved by direct methods and refined by full-matrix least squares on F^2. All hydrogen atoms were placed in calculated positions. Structure solution and refinement were performed by using the SHELXL-97 package.[18] Details of the X-ray structure determinations and refinements are provided in Table 1.

Table 1 Crystal data and structure refinement for **Ni1'** and **Ni3**

	Ni1'	**Ni3**
Empirical formula	$C_{18}H_{26}Br_2N_2NiO_3$	$C_{44}H_{56}Br_4N_4Ni_2$
Formula weight	536.93	1077.99
Temperature/K	173 (2)	173 (2)
Wavelength/Å	0.71073	0.71073
Crystal system	triclinic	triclinic
space group	P-1	P-1
a/Å	8.2799 (17)	9.6080 (19)
b/Å	8.7003 (17)	12.672 (3)
c/Å	15.655 (3)	18.524 (4)
α/°	76.36 (3)	103.25 (3)
β/°	80.94 (3)	91.58 (3)
γ/°	75.15 (3)	99.53 (3)
Volume/Å^3	1053.7 (4)	2160.0 (7)
Z	2	2
D_{calcd}/(g cm^{-3})	1.689	1.657
μ/mm^{-1}	4.732	4.607
F(000)	538.0	1088.0
Crystal size/mm	0.489 × 0.243 × 0.115	0.303 × 0.207 × 0.182
θ range/°	4.94 to 54.98	2.26 to 54.96
Limiting indices	-10 ≤ h ≤ 10 -11 ≤ k ≤ 11 -20 ≤ l ≤ 20	-12 ≤ h ≤ 12 -16 ≤ k ≤ 16 -24 ≤ l ≤ 24
No. of rflns collected	10399	24079
No. unique rflns [R(int)]	4709 (0.0415)	9706 (0.0214)
Completeness to θ	97.0%	98.0%
Data/restraints/parameters	4709/0/250	9706/0/509
Goodness of fit on F^2	1.071	1.066
Final R indices [$I>2\Sigma(I)$]	R_1 = 0.0372 wR_2 = 0.0887	R_1 = 0.0277 wR_2 = 0.0672
R indices (all data)	R_1 = 0.0340 wR_2 = 0.0900	R_1 = 0.0300 wR_2 = 0.0686
Largest diff. peak and hole (e Å^{-3})	0.88/-0.77	0.65/-0.61

The SQUEEZE option of the crystallographic program PLATON was used to remove free solvent from the structures of **Ni1'** and **Ni3**. Details of the X-ray structure determinations and refinements are provided in Table 1. CCDC 1554536 (**Ni1'**) and 1554537(**Ni3**.) contain the crystallographic data for this article, which could be obtained free of charge from the Cambridge Crystallographic Data Centre via www.ccdc.cam.ac.uk/ data_request/cif.

RESULTS AND DISCUSSION

Synthesis and characterization Reaction of the imino-cyclopenta[*b*]pyridines, 7-(ArN)-6-Me$_2$C$_8$H$_5$N (Ar = 2,6-Me$_2$C$_6$H$_3$ (**L1**), 2,6-Et$_2$C$_6$H$_3$ (**L2**), 2,6-*i*-Pr$_2$C$_6$H$_3$ (**L3**), 2,4,6-Me$_3$C$_6$H$_2$ (**L4**), 2,6-Et$_2$-4-MeC$_6$H$_2$ (**L5**)), with NiBr$_2$(DME) in dichloromethane affords the corresponding nickel complexes, [7-(ArN)-6-Me$_2$C$_8$H$_5$N]NiBr$_2$ (**Ni1** - **Ni5**) in excellent yields (Scheme 1). The synthetic procedures for **L1** – **L5**, involving the condensation of 2-chloro-6,6-dimethyl-cyclopenta[*b*]pyridin-7-one with the corresponding aniline, have been reported previously.[16] All five complexes have been characterized using IR spectroscopy and

elemental analysis while **Ni1** and **Ni3** have been the subject of single crystal X-ray diffraction studies.

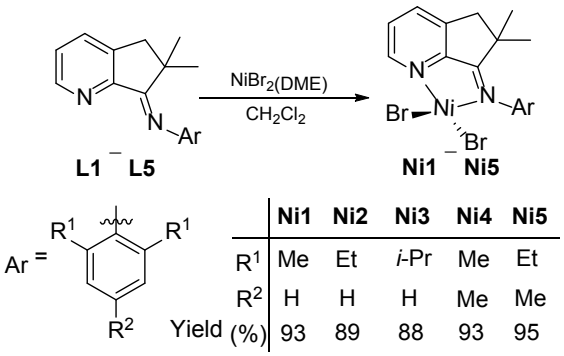

	Ni1	Ni2	Ni3	Ni4	Ni5
R^1	Me	Et	*i*-Pr	Me	Et
R^2	H	H	H	Me	Me
Yield (%)	93	89	88	93	95

Scheme 1 Synthetic procedure for **Ni1 – Ni5**

Single crystals of **Ni1** and **Ni3** suitable for X-ray determination were grown by slow diffusion of diethyl ether into a dichloromethane solution of the corresponding complex at room temperature. The molecular structures are shown in Figs. 1 and 2, respectively; selected bond lengths and angles are compiled in Table 2 Examination of the structure shown in Fig. 1, reveals a cation-anion pair of composition [**L1**NiBr$(OH_2)_3$][Br] (**Ni1'**). Its apparent that one of the bromide ligands in **Ni1** has dissociated with the result that it now acts a non-coordinating anion, while three molecules of water are bound to the remaining cationic nickel center. The distorted octahedral geometry in **Ni1'** at nickel is completed by the two nitrogen donors belonging to **L1** and the remaining bromide ligand. Two of the water molecules are mutually trans (O2–Ni1–O3 175.09(6)°), while the other is trans to the pyridine nitrogen. The Ni–$N_{pyridine}$ bond (2.0693(19) Å) is shorter than the Ni–N_{imino} one (2.1670(2) Å), in a manner similar to that observed for analogous nickel complexes.[11d,12b,15] The plane of the N_{imino}-aryl ring is inclined toward perpendicular with respect to the plane comprising N1, N2 and Ni1 with a dihedral angle of 87.24°.

Table 2 Selected bond lengths (Å) and angles (°) for **Ni1'** and **Ni3**

Ni1'		**Ni3**	
Bond lengths (Å)			
Ni(1)–N(1)	2.1670(2)	Ni(1)–N(1)	2.1454(15)
Ni(1)–N(2)	2.0693(19)	Ni(1)–N(2)	2.0555(15)
Ni(1)–Br(1)	2.5771(9)	Ni(1)–Br(1)	2.5186(8)
Ni(1)–O(1)	2.0443(17)	Ni(1)–Br(1^i)	2.5080(7)
Ni(1)–O(2)	2.0718(16)	Ni(1)–Br(2)	2.4032(8)
Ni(1)–O(3)	2.0789(16)		
Bond angles (°)			
N(1)–Ni(1)–N(2)	81.29(8)	Br(1)–Ni(1)–O(3)	88.48(5)
N(1)–Ni(1)–Br(1)	178.36(5)	O(2)–Ni(1)–O(3)	175.09(6)
N(1)–Ni(1)–O(1)	88.22(7)	N(1)–Ni(1)–N(2)	81.01(6)
N(1)–Ni(1)–O(2)	92.28(7)	N(1)–Ni(1)–Br(1)	141.40(4)
N(1)–Ni(1)–O(3)	92.34(7)	N(1)–Ni(1)–Br(2)	104.59(4)
N(2)–Ni(1)–Br(1)	97.32(6)	N(1)–Ni(1)–Br(1^i)	95.50(4)
N(2)–Ni(1)–O(1)	169.16(7)	N(2)–Ni(1)–Br(1)	90.41(5)
N(2)–Ni(1)–O(2)	90.87(7)	N(2)–Ni(1)–Br(2)	90.17(5)
N(2)–Ni(1)–O(3)	88.17(7)	N(2)–Ni(1)–Br(1^i)	169.01(4)
Br(1)–Ni(1)–O(1)	93.20(6)	Br(1)–Ni(1)–Br(2)	113.06(3)
Br(1)–Ni(1)–O(2)	86.87(5)		

The 'i' atoms have been generated by symmetry.

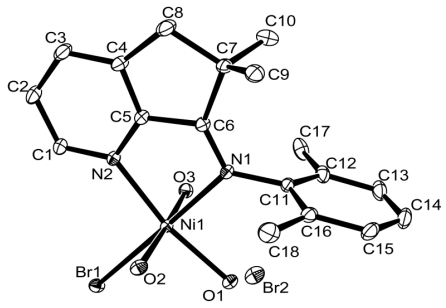

Fig. 1 ORTEP representation of cation-anion pair **Ni1'** with the thermal ellipsoids at 30% probability level; the H atoms are omitted for clarity.

Unlike **Ni1**, no adventitious reaction with water occurs on crystallization of **Ni3**. Instead **Ni3** adopts a dimeric structure in which two bromide ligands bridge the metal centers while the other two bromides act as monodentate ligands. The five-coordinate geometry at each metal center is completed by the two nitrogen donors belonging to **L3**. Bromide-bridged structures are a well-known motif for N^N-nickel(II) halide complexes and indeed **Ni3** displays similar features to these literature reports.[11a,11b,11c,12a,16,19] The five-coordinate geometry at each nickel center can be best described as distorted square-pyramidal

geometry with Br2 forming the apex and N1, N2, Br1 and Br1^{i} the square base. As with **Ni1'**, the Ni–N_{imino} bond (2.1454(15) Å) is noticeably longer than the Ni–$N_{pyridine}$ (2.0555(15) Å) distance, while the N-aryl group is again oriented almost perpendicular to the plane defined by N1, N2 and Ni1 (dihedral angle of 83.53).

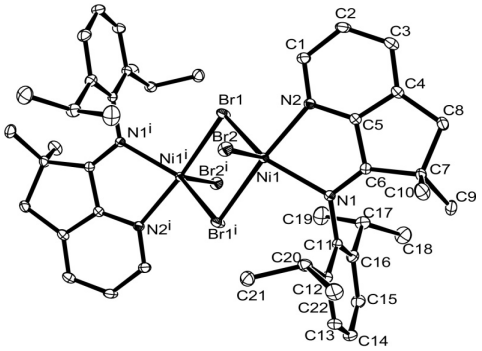

Fig. 2 ORTEP representation of complex **Ni3** with the thermal ellipsoids at 30% probability level; the H atoms are omitted for clarity.

All the complexes, **Ni1** – **Ni5**, display $\nu_{C=N}$ stretching vibrations in the range of 1630 – 1635 cm^{-1} in their IR spectra which compares to 1672 – 1680 cm^{-1} for the free ligands.[16] This shift to lower wavenumber is consistent with effective coordination between the nickel and the imine nitrogen atom. Moreover, the microanalytical data for **Ni1** – **Ni5** are consistent with the proposed elemental composition.

Ethylene Polymerization

With the intention of determining the most suitable co-catalyst, **Ni4** was, in the first instance, explored as the test pre-catalyst with four different alkylaluminum reagents including methylaluminoxane (MAO), modified methylaluminoxane (MMAO), ethylaluminum sesquichloride ($Et_3Al_2Cl_2$, EASC) and diethylaluminum chloride (Et_2AlCl). Typically the runs were performed at 30 ºC under 10 atmospheres of ethylene pressure; the results are collected in Table 3. As a general observation all co-catalysts gave good activities for the polymerization with the values falling in the range 1.25 – 3.55 x 10^6 g(PE)·mol^{-1}(Ni)·h^{-1}.

Table 3 Identification of the most suitable co-catalyst using **Ni4**[a]

Entry	Co-cat.	Al/Ni	Act.[b]	T_m[c]/ºC	M_w[d]	M_w/M_n[d]
1	MAO	2000	1.25	97.2	1.25	1.53
2	MMAO	2000	3.11	97.7	1.16	1.47
3	Et_2AlCl	500	3.51	71.1	0.87	1.39
4	EASC	500	1.86	80.0	1.03	1.43

[a] Reaction conditions: 3 μmol **Ni4**, 30 ºC, 30 min., 10 atm ethylene, 100 mL toluene; [b] 10^6 g(PE)·mol^{-1}(Ni)·h^{-1}; [c] Determined by DSC; [d] Determined by GPC and and M_w:kg mol^{-1} .

With MMAO and Et_2AlCl proving the most conducive to high activity, these two co-catalysts were selected for subsequent more detailed investigations. All polymers were characterized by gel permeation chromatography (GPC) and by differential scanning calorimetry (DSC).

Polymerization screen using Ni1 – Ni5/MMAO

With MMAO as the co-catalyst, **Ni4** was used to establish the optimal Al/Ni molar ratio, reaction temperature and reaction time; the results are listed in Table 4. Firstly, the effect of varying the molar ratios of Al/Ni from 1500 to 2500 on **Ni4** was examined with the temperature set at 30 ºC and the run time at 30 minutes (entries 1 – 5, Table 4). Inspection of the data reveals the highest activity of 3.88 × 10^6 g(PE)·mol^{-1}(Ni)·h^{-1} is obtained with an Al/Ni molar ratio at 1750 (entry 2, Table 4). After this point the activity gradually decreases as the Al/Ni molar ratio increases. However, in contrast to many related nickel catalysts,[11d,20] there is a perceptible increase in the molecular weight of the polyethylenes as the Al/Ni ratio increases, implying enhanced chain propagation over termination (Fig. 3); such a phenomenon has some limited precedent with nickel.[21]

Secondly, with the Al/Ni molar ratio fixed at 1750, the temperature of the run was increased in ten degree increments from 20 to 50 °C (entries 2, 6 – 8, Table 4). The optimum temperature was observed as 30 °C (entry 2, Table 4). Raising the temperature further resulted in a sharp decrease in activity, this being attributed

Table 4 Polymerization of ethylene in the presence of MMAO[a]

Entry	Precat.	Al/Ni	*T*/°C	*t*/min	PE/g	Activity[b]	T_m[c]/°C	M_w[d]/Kg·mol^{-1}	M_w/M_n[d]
1	**Ni4**	1500	30	30	3.98	2.65	97.7	1.12	1.47
2	**Ni4**	1750	30	30	5.82	3.88	95.6	1.11	1.43
3	**Ni4**	2000	30	30	4.67	3.11	97.7	1.16	1.47
4	**Ni4**	2250	30	30	3.77	2.51	98.4	1.19	1.46
5	**Ni4**	2500	30	30	3.33	2.22	98.7	1.21	1.47
6	**Ni4**	1750	20	30	5.56	3.71	99.6	1.24	1.53
7	**Ni4**	1750	40	30	3.50	2.33	90.2	0.91	1.36
8	**Ni4**	1750	50	30	1.28	0.85	90.0	0.89	1.29
9	**Ni4**	1750	30	15	1.55	2.07	97.2	1.16	1.38
10	**Ni4**	1750	30	45	7.10	3.15	96.1	1.12	1.46
11	**Ni4**	1750	30	60	8.13	2.71	95.5	1.04	1.46
12	**Ni1**	1750	30	30	3.84	2.56	95.3	0.93	1.42
13	**Ni2**	1750	30	30	1.74	1.16	90.1	0.81	1.30
14	**Ni3**	1750	30	30	trace	-	-	-	-
15	**Ni5**	1750	30	30	1.94	1.29	92.1	0.92	1.30
16[e]	**Ni4**	1750	30	30	1.57	1.05	91.0	1.01	1.42

[a] Reaction conditions: 3 μmol Ni, 10 atm. ethylene, 100 mL toluene; [b] 10^6 g(PE)·mol^{-1}(Ni)·h^{-1}; [c] Determined by DSC; [d] Determined by GPC; [e] 5 atm. ethylene

to both the instability of the active species and the lower solubility of ethylene in toluene at higher temperature.[4a,11a,17c,22]

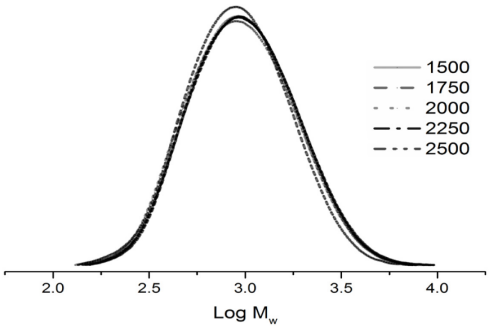

Fig. 3 GPC curves for the polyethylenes obtained using **Ni4**/MMAO with various Al/Ni ratios (entries 1 – 5, Table 4).

Moreover, with respect to the properties of the polyethylenes, the GPC curves clearly indicate that the polyethylene gradually lowers in molecular weight as the reaction temperature is raised (Fig. 4). This observation would suggest more facile chain transfer and termination at the higher temperature.[11,12] Similar correlations with reaction temperature can be observed with melting temperature (T_m) of the polymer and molecular weight distribution.

Thirdly, with the temperature set at 30 °C and the Al/Ni ratio at 1750, the lifetime of active species was investigated. Monitoring the polymerization over run times of 15, 30, 45 and 60 minutes (entries 2, 9 – 11, Table 4), the activity reached a peak at 3.88 x 10^6 g(PE)·mol^{-1}(Ni)·h^{-1} after 30 minutes (entry 2, Table 4).

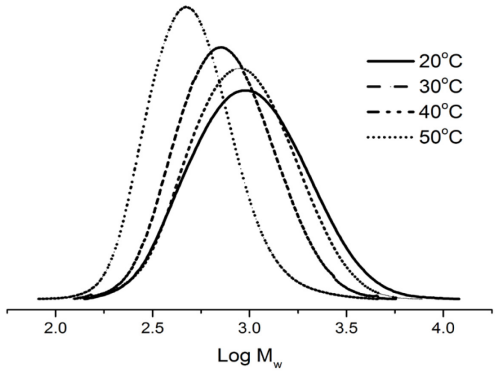

Fig. 4 GPC curves for the polyethylenes obtained using **Ni4**/MMAO at different temperatures (entries 2, 6 – 8, Table 4).

Beyond 30 minutes the activity gradually decreased reaching a minimum of 2.71 x 10^6 g(PE)·mol^{-1}(Ni)·h^{-1} after 60 minutes (entry 11, Table 4). This steady decrease in activity is likely due to partial deactivation of the active species.[23] Although an alternative explanation may be due to the increased viscosity of the reaction medium over time as more polymer is generated hence limiting the diffusion of ethylene to the active species.[21a]

Finally, with the optimized conditions established (Al/Ni ratio 1750, run temperature of 30 °C and a run time of 30 minutes) the other pre-catalysts **Ni1**, **Ni2**, **Ni3** and **Ni5** were

screened for ethylene polymerization (entries 12 – 15, Table 4). On inspection of the data the activities of these four catalysts along with **Ni4** follow the order: **Ni4** [2,4,6-tri(Me)] > **Ni1** [2,6-di(Me)] > **Ni5** [2,6-di(Et)-4-Me] > **Ni2** [2,6-di(Et)] >> **Ni3** [2,6-di(*i*-Pr)]. In general, less sterically hindered pre-catalysts with electron donating groups at the *para*-position favor good catalytic efficiency.[24] The improved solubility of the *para*-methylated complexes, **Ni4** and **Ni5**, in toluene may also account for better catalytic activities.[11(a)] Surprisingly, **Ni3** containing the bulky *o*-substituents (*i*-Pr) showed very low activity (entry 14, Table 4), an observation that can likely be attributed to the sterically hindered *o*-substituents blocking the ethylene monomer from approaching the active center.[25]

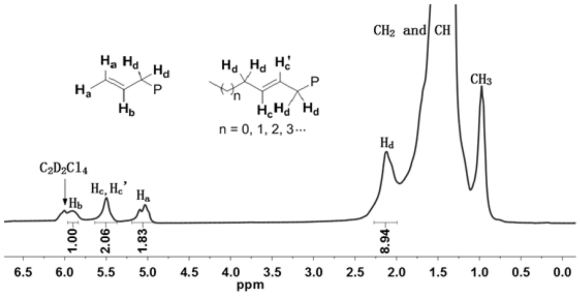

Fig. 5 ^{1}H NMR spectrum of the polyethylene obtained using **Ni4/**MMAO (entry 2, Table 4); recorded in $C_2Cl_4D_2$

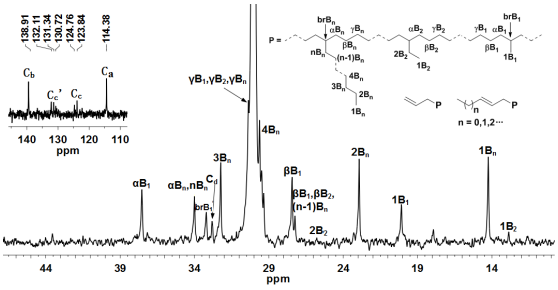

Fig. 6 ^{13}C NMR spectrum of the polyethylene obtained using **Ni4/**MMAO (entry 2, Table 4); recorded in $C_2Cl_4D_2$

To investigate the microstructure of these polyethylenes a representative sample generated using **Ni4**/MMAO was characterized by high-temperature ^{1}H NMR, ^{13}C NMR and DEPT135 NMR spectroscopy (recorded in deuterated 1,1,2,2-tetrachloroethane ($C_2Cl_4D_2$) at 100 °C). Two downfield peaks δ 5.90 and δ 5.00 in the ^{1}H NMR spectrum (Fig. 5) along with peaks around δ 114.7 and 139.9 in the ^{13}C NMR spectrum (Fig. 6) support the presence of a vinyl end-group (-CH=CH$_2$).[25] In addition, peaks at δ 5.49 in ^{1}H NMR spectrum are consistent with the presence of internal vinylene groups (-CH=CH-) which is corroborated by signals at δ 131.0 and 124.0 in the ^{13}C NMR spectrum.[27] Further evidence for these assignments is provided by the DEPT135 NMR spectrum (Fig. 7), which shows three positive peaks around 139.0, 131.0 and 123.1 ppm and one negative peak at 114.1 ppm. Similar microstructural properties have been noted in the polyethylenes obtained using the 7-arylimino-6,6dimethyl-cyclopenta[*b*]pyridyl-nickel chlorides (**E**, Chart 1); a related mechanism to that proposed previously

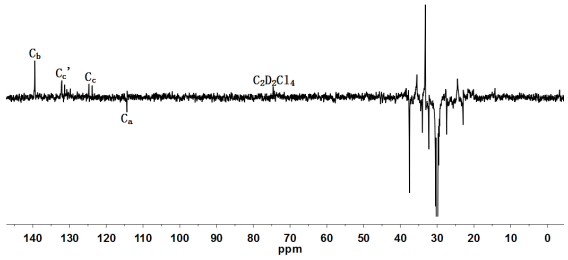

Fig. 7 DEPT135 NMR spectrum of the polyethylene obtained using **Ni4/**MMAO (entry 2, Table 4); recorded in $C_2Cl_4D_2$

would seem likely to account for the structural features.[16] A branching analysis was also performed on the polymer using the data acquired from the ^{13}C NMR spectrum using methods previously reported.[27b,28] Typically this analysis revealed 34 branches per 1000 carbons and includes 28.0% methyl branches, 5.1% ethyl branches and 66.9% longer chain branches.

Polymerization screen using Ni1 – Ni5/Et$_2$AlCl

To explore in more detail the use of Et$_2$AlCl as the co-catalyst, **Ni4** was again selected as the test pre-catalyst to ascertain the optimum polymerization parameters to deliver the best activity for the polymerization; the results are

assembled in Table 5. As a general point, the data reveal similar activities to that observed with MMAO as co-catalyst, however, the polyethylene obtained displays lower molecular weight and narrower molecular weight distributions.

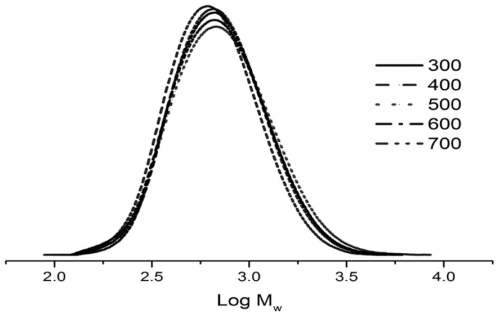

Fig. 8 GPC curves for the polyethylenes obtained using **Ni4**/Et_2AlCl with various Al/Ni ratios (entries 1 – 5, Table 5).

Firstly, the effect of varying the molar ratio of Al/Ni on the catalytic activity of **Ni4** and other polymer properties was investigated. Typically, the Al/Ni ratio was varied from 300 up to 700 with the temperature set at 30 °C and the run time at 30 minutes (entries 1 − 5, Table 5). Examination of the data reveals a peak activity of 3.51 × 10^6 g(PE) mol^{-1}(Ni) h^{-1} at an Al/Ni ratio of 500 (entry 3); in addition this ratio also delivers the highest molecular weight of 0.87 Kg mol^{-1} for these 5 runs. Above 500 the catalytic activities and molecular weight slightly decrease; the molecular weight variation across the five ratios is depicted in the GPC curves in Fig. 8.

Secondly, with the Al/Ni ratio maintained at 500 the effect of increasing the reaction temperature from 20 to 50 ºC using **Ni4** was explored (entries 3, 6 − 8, Table 5). As with the **Ni4**/MMAO system, the highest activity of 3.51 × 10^6 g(PE) mol^{-1}(Ni) h^{-1} were reached at 30 ºC (entry 3, Table 5) above which the activities lowered and quite sharply at 50 °C (entry 8, Table 5). At the same time the molecular weight and the T_m values of the polymer all decreased (Fig. 9).

Thirdly, with the Al/Ni molar ratio fixed at 500 and the reaction temperatures of 30 °C, the

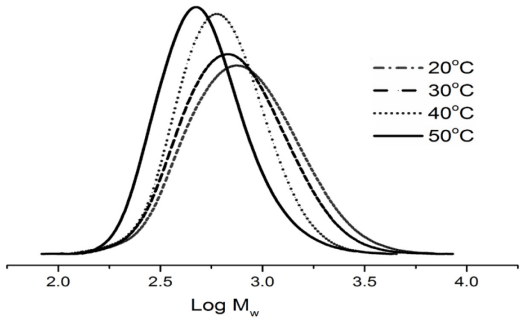

Fig. 9 GPC curves for the polyethylenes obtained using **Ni4**/Et_2AlCl at different temperatures (entries 3, 6 – 8, Table 5).

polymerization run using **Ni4** was terminated at 5, 10, 15, 30, 45, 60 and 120 minutes (entries 3, 9 − 14, Table 5). As with the earlier study the maximum activity (3.51 × 10^6 g(PE) mol^{-1}(Ni) h^{-1}) was observed after 30 minutes (entry 3, Table 5). Nevertheless, a remarkably smooth profile (in the range 3.28 − 3.51 × 10^6 g(PE)·mol^{-1}(Ni)·h^{-1}) for the activity was observed from 10 to 60 minutes. Even after 120 minutes the activity had only fallen to 2.12 × 10^6 g(PE)·mol^{-1}(Ni)·h^{-1}). However, the low activity observed after 5 minutes (entry 9, Table 5) implies there is an induction period of about 10 minutes to fully generate the active species before the catalyst reaches its optimal performance. Following optimization of the conditions for **Ni4**/Et_2AlCl, the remaining four pre-catalysts were then investigated with an Al/Ni ratio 500, run temperature of 30 °C and a run time of 30 minutes (entries 3, 15 − 18, Table 5). In terms of catalytic activity the pre-catalysts fall in the order: **Ni4** [2,4,6-tri(Me)] > **Ni1** [2,6-di(Me)] > **Ni5** [2,6-di(Et)-4-Me] > **Ni2** [2,6-di(Et)] >> **Ni3** [2,6-di(*i*-Pr)]. This order mimics that seen in the study with MMAO with **Ni3** again showing very low activity and highlighting the preference for low steric bulk and electron donating *para*-substituents. Of the five pre-catalysts screened, **Ni1** gives the lowest molecular weight of 0.67Kg·mol^{-1} and **Ni4** the highest of 0.87 $Kgmol^{-1}$ (entries 3 and 15, Table 5).

Table 5 Catalytic evaluation using Et_2AlCl as co-catalyst[a]

Entry	Precat.	Al/Ni	*T*/°C	*t*/min	PE/g	Activity[b]	T_m[c]/°C	M_w[d]/Kg·mol^{-1}	M_w/M_n[d]
1	**Ni4**	300	30	30	2.95	1.97	67.5	0.81	1.33
2	**Ni4**	400	30	30	4.47	2.98	69.0	0.81	1.33
3	**Ni4**	500	30	30	5.26	3.51	71.1	0.87	1.39
4	**Ni4**	600	30	30	5.15	3.43	71.1	0.82	1.36
5	**Ni4**	700	30	30	4.49	2.99	64.6	0.75	1.31
6	**Ni4**	500	20	30	4.53	3.02	88.6	0.97	1.43
7	**Ni4**	500	40	30	3.42	2.28	64.8	0.71	1.27
8	**Ni4**	500	50	30	1.30	0.87	63.5	0.70	1.27
9	**Ni4**	500	30	5	0.47	1.88	72.1	0.84	1.28
10	**Ni4**	500	30	10	1.64	3.28	71.2	0.80	1.29
11	**Ni4**	500	30	15	2.49	3.32	69.1	0.80	1.29
12	**Ni4**	500	30	45	7.69	3.42	66.2	0.77	1.38
13	**Ni4**	500	30	60	10.02	3.34	75.2	0.76	1.40
14	**Ni4**	500	30	120	12.74	2.12	71.6	0.82	1.39
15	**Ni1**	500	30	30	4.62	3.08	64.1	0.67	1.32
16	**Ni2**	500	30	30	1.52	1.01	70.6	0.75	1.23
17	**Ni3**	500	30	30	trace	-	-	-	-
18	**Ni5**	500	30	30	2.18	1.45	65.9	0.73	1.25
19[e]	**Ni4**	500	30	30	2.35	1.57	66.1	0.79	1.32

[a] Reaction conditions: 3 μmol Ni, 10 atm ethylene, 100 mL toluene; [b] 10^6 g(PE)·mol^{-1}(Ni)·h^{-1}; [c] Determined by DSC; [d] Determined by GPC; [e] 5 atm ethylene

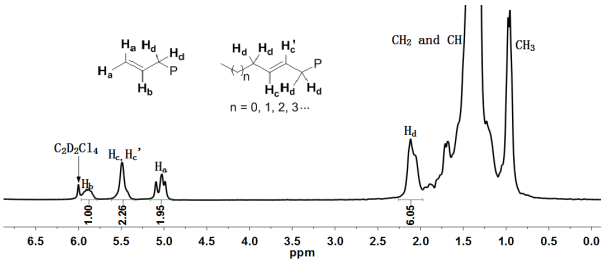

Fig. 10 ^{1}H NMR spectrum of the polyethylene obtained using **Ni4**/Et_2AlCl (entry 3, Table 5); recorded in $C_2Cl_4D_2$

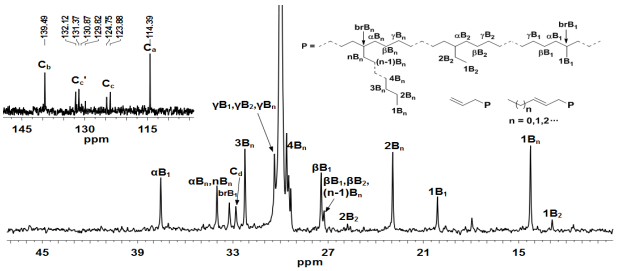

Fig. 11 ^{13}C NMR spectrum of the polyethylene obtained using **Ni4**/Et_2AlCl (entry 3, Table 5); recorded in $C_2Cl_4D_2$

To confirm the expected structural properties of the polyethylene obtained with this co-catalyst, a sample of the material obtained using **Ni4**/Et_2AlCl (entry 3, Table 5) was subjected to a high-temperature ^{1}H NMR, ^{13}C NMR and DEPT135 NMR spectroscopic study (Figs. 10 – 12). Once again, the data reveal the existence of

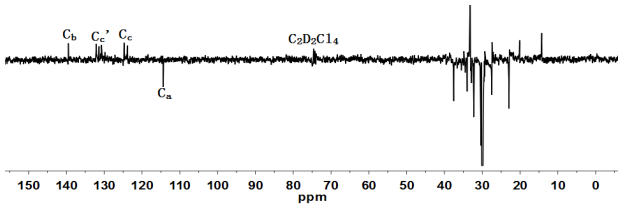

Fig. 12 DEPT135 NMR spectrum of the polyethylene obtained using **Ni4**/Et_2AlCl (entry 3, Table 5); recorded in $C_2Cl_4D_2$

unsaturated vinyl and vinylene groups. In addition, the branching analysis based on the ^{13}C NMR data shows 41 branches/1000 carbons, including 26.2% methyl branches, 6.3% ethyl branches and 67.5% longer chain branches, which is comparable to that seen using Ni4/MMAO (*vide supra*).[27b,28]

Overall, it is apparent that the active bromide-containing pre-catalysts (**Ni1**, **Ni2**, **Ni4**, **Ni5**) developed in this work form similar low molecular weight polymeric material to that seen using chloride-containing **E** (Chart 1), albeit with slightly lower activity. However, closer inspection of the data reveal that the current systems show that the absolute molecular weight is lower (as low as 0.67 Kg·mol^{-1}). Indeed, when compared with other cycloalkyl-fused iminopyridyl-nickel pre-catalysts (**A** – **E**, Chart 1), the current systems afford the lowest molecular weight

polyethylene for this class of nickel pre-catalyst (Chart 2).

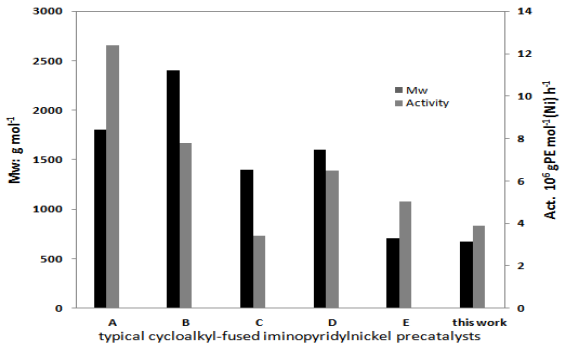

Chart 2 The catalytic performances of cycloalkyl-fused iminopyridyl-nickel pre-catalysts (**A** – **E** and this work)

Conclusions

Five related imino-cyclopenta[*b*]pyridyl-nickel(II) bromides (**Ni1** – **Ni5**), differing in the steric and electronic properties of the *N*-aryl group, were synthesized and fully characterized; the molecular structures of **Ni1'** and **Ni3** were also determined. **Ni1**, **Ni2**, **Ni4** and **Ni5** all proved highly active catalysts for the ethylene polymerization on activation with MMAO or Et_2AlCl (up to 3.88 × 10^6 g(PE)·mol^{-1}(Ni)·h^{-1}). Steric and electronic factors play key roles in dictating catalytic performance with the least sterically protected pre-catalyst containing an electron-donating group Me at the *para* position (**Ni4**) delivering the best performance; by contrast the most sterically hindered system (**Ni3**) showed scarcely any activity. The waxy polyethylenic materials obtained display low molecular weights, narrow molecular weight distributions and contain unsaturated vinyl and vinylene units. Such materials have shown some demand as long-chain branched co-monomers, functionally modifiable polymers as well as for coating materials.

Acknowledgements

This work was supported by National Natural Science Foundation of China (Nos. U1362204, 21473160, and 21374123). GAS thanks the Chinese Academy of Sciences for a visiting fellowship.

References

1. L. K. Johnson, C. M. Killian, M. Brookhart, *J. Am. Chem. Soc.*, **1995**, 117, 6414–6415.
2. (a) C. S. Popeney, A. L. Rheingold, Z. Guan, *Organometallics*, **2009**, 28, 4452–4463; (b) D. H. Leung, J. W. Ziller, Z. Guan, *J. Am. Chem. Soc.*, **2008**, 130, 7538–7539; (c) T. V. Laine, K. Lappalainen, J. Liimatta, E. Aitola, B. Lofgren, M. Leskela, *Macromol. Rapid Commun.*, **1999**, 20, 487–491; (d) A. Koppl, H. G. Alt, *J. Mol. Catal. A: Chem.*, **2000**, 154, 45–53; (e) S. D. Ittel, L. K. Johnson, M. Brookhart, *Chem. Rev.*, **2000**, 100, 1169–1203; (f) S. Mecking, *Coord. Chem. Rev.*, **2000**, 203, 325–351.
3. (a) W.-H. Sun, *Adv. Polym. Sci.*, **2013**, 258, 163–178; (b) R. Gao, W.-H. Sun, C. Redshaw, *Catal. Sci. Technol.*, **2013**, 3, 1172–1179; (c) S. Wang, W.-H. Sun, C. Redshaw, *J. Organomet. Chem.*, **2014**, 751, 717–741; (d) C. Bianchini, G. Giambastiani, L. Luconi, A. Meli, *Coord. Chem. Rev.*, **2010**, 254, 431–455.
4. (a) S. A. Svejda, M. Brookhart, *Organometallics*, **1999**, 18, 65–74; (b) T. V. Laine, U. Piironen, K. Lappalainen, M. Klinga, E. Aitola, M. Leskelä, *J. Organomet. Chem.*, **2000**, 606, 112–124; (c) C. Shao, W.-H. Sun, Z. Li, Y. Hu, L. Han, *Catal. Commun.*, **2002**, 3, 405–410; (d) S. Jie, D. Zhang, T. Zhang, W.-H. Sun, J. Chen, Q. Ren, D. Liu, G. Zheng, W. Chen, *J. Organomet. Chem.*, **2005**, 690, 1739–1749; (e) C. Zhang, W.-H. Sun, Z.-X. Wang, *Eur. J. Inorg. Chem.*, **2006**, 4895–4902; (f) R. Gao, L. Xiao, X. Hao, W.-H. Sun, F. Wang, *Dalton Trans.*, **2008**, 5645–5651; (g) F. Yang, Y. Chen, Y. Lin, K. Yu, Y. Liu, Y. Wang, S. Liu, J.-T. Chen, *Dalton Trans.*, **2009**, 1243–1250.
5. (a) C. Wang, S. Friedrich, T. R. Younkin, R. T. Li, R. H. Grubbs, D. A. Bansleben, M. W. Day, *Organometallics*, **1998**, 17, 3149–3151; (b) C. Carlini, M. Isola, V. Liuzzo, A. M. R. Galletti, G. Sbrana, *Appl. Catal., A*, **2002**,

231, 307–320; (c) S. Wu, S. Lu, *Appl. Catal., A*, **2003**, 246, 295–301; (d) F. Chang, D. Zhang, G. Xu, H. Yang, J. Li, H. Song, W.-H. Sun, *J. Organomet. Chem.*, **2004**, 689, 936–946; (e) T. Hu, L.-M. Tang, X.-F. Li, Y.-S. Li, N.-H. Hu, *Organometallics*, **2005**, 24, 2628–2632.

6. (a) W. Keim, S. Killat, C. F. Nobile, G. P. Suranna, U. Englert, R. Wang, S. Mecking, D. L. Schröder, *J. Organomet. Chem.*, **2002**, 662, 150–171; (b) W.-H. Sun, Z. Li, H. Hu, B. Wu, H. Yang, N. Zhu, X. Leng, H. Wang, *New J. Chem.*, **2002**, 26, 1474–1478; (c) F. Speiser, P. Braunstein, L. Saussine, R. Welter, *Organometallics*, **2004**, 23, 2613–2624; (d) F. Speiser, P. Braunstein, L. Saussine, *Organometallics*, **2004**, 23, 2625–2632; (e) F. Speiser, P. Braunstein, L. Saussine, R. Welter, *Inorg. Chem.*, **2004**, 43, 1649–1658; (f) Z. Weng, S. Teo, T. S. A. Hor, *Organometallics*, **2006**, 25, 4878–4882.
7. (a) L. Wang, W.-H. Sun, L. Han, H. Yang, Y. Hu, X. Jin, *J. Organomet. Chem.*, **2002**, 658, 62–70; (b) N. Ajellal, M. C. A. Kuhn, A. D. G. Boff, M. Hörner, C. M. Thomas, J.-F. Carpentier, O. L. Casagrande, *Organometallics*, **2006**, 25, 1213–1216; (c) S. Adewuyi, G. Li, S. Zhang, W. Wang, P. Hao, W.-H. Sun, N. Tang, J. Yi, *J. Organomet. Chem.*, **2007**, 692, 3532–3541; (d) M. Zhang, S. Zhang, P. Hao, S. Jie, W.-H. Sun, P. Li, X. Lu, *Eur. J. Inorg. Chem.*, **2007**, 3816–3826.
8. F. Speiser, P. Braunstein, L. Saussine, *Dalton Trans.*, **2004**, 1539–1545.
9. (a) X. Tang, W.-H. Sun, T. Gao, J. Hou, J. Chen, W. Chen, *J. Organomet. Chem.*, **2005**, 690, 1570–1580; (b) Q.-Z. Yang, A. Kermagoret, M. Agostinho, O. Siri, P. Braunstein, *Organometallics*, **2006**, 25, 5518–5527.
10. P. Braunstein, Y. Chauvin, S. Mercier, L. Saussine, *C. R. Chim.*, **2005**, 8, 31–38.
11. (a) J. Yu, Y. Zeng, W. Huang, X. Hao, W.-H. Sun, *Dalton Trans.*, **2011**, 40, 8436–8443; (b) X. Hou, Z. Cai, X. Chen, L. Wang, C. Redshaw, W.-H. Sun, *Dalton Trans.*, **2012**, 41, 1617–1623; (c) L. Zhang, X. Hao, W.-H. Sun, C. Redshaw, *ACS Catal.*, **2011**, 1, 1213–1220; (d) Z. Sun, E. Yue, M. Qu, I. V. Oleynik, I. I. Oleynik, K. Li, T. Liang, W. Zhang, W.-H. Sun, *Inorg. Chem. Front.*, **2015**, 2, 223–227.
12. (a) F. Huang, Z. Sun, S. Du, E. Yue, J. Ba, X. Hu, T. Liang, G. B. Galland, W.-H. Sun, *Dalton Trans.*, **2015**, 44, 14281–14292; (b) Z. Sun, F. Huang, M. Qu, E. Yue, I. V. Oleynik, I. I. Oleynik, Y. Zeng, T. Liang, K. Li, W. Zhang, W.-H. Sun, *RSC Adv.*, **2015**, 5, 77913–77921.
13. R. Zhang, Z. Wang, Z. Flisak, X. Hao, Q. Liu, W.-H. Sun, *J. Polym. Sci., Part A: Polym. Chem.*, **2017**, 55, 2501-2610.
14. (a) J. Ba, S. Du, E. Yue, X. Hu, Z. Flisak, W.-H. Sun, *RSC Adv.*, **2015**, 5, 32720–32729; (b) Y. Zhang, C. Huang, X. Hao, X. Hu, W.-H. Sun, *RSC Adv.*, **2016**, 6, 91401–91408.
15. C. Huang, Y. Zhang, T. Liang, Z. Zhao, X. Hu, W.-H. Sun, *New J. Chem.*, **2016**, 40, 9329–9336.
16. Y. Zhang, C. Huang, X. Wang, Q. Mahmood, X. Hao, X. Hu, C.-Y. Guo, G. A. Solan, W.-H. Sun, *Polym. Chem.*, **2017**, 8, 995–1005.
17. (a) D. Zhang, E. T. Nadres, M. Brookhart, O. Daugulis, Organometallics, **2013**, 32, 5136–5143; (b) D. H. Camachoa, Z. Guan, *Chem. Commun.*, **2010**, 46, 7879–7893; (c) Z. Flisak, W.-H. Sun, ACS Catal., **2015**, 5, 4713–4724.
18. G. M. Sheldrick, *SHELXTL-97, Program for the Refinement of Crystal Structures*, University of Göttingen, Germany, **1997**
19. (a) J. Yu, X. Hu, Y. Zeng, L. Zhang, C. Ni, X. Hao, W.-H. Sun, *New J. Chem.*, **2011**, 35, 178–183; (b) W. Chai, J. Yu, L. Wang, X. Hu, C. Redshaw, W.-H. Sun, *Inorg. Chim. Acta.*, **2012**, 385, 21–26.
20. (a) C. Wen, S. Yuan, Q. Shi, E. Yue, D. Liu, W.-H. Sun, *Organometallics*, **2014**, 33, 7223−7231; (b) S. Du, Q. Xing, Z. Flisak, E. Yue, Y. Sun, W.-H. Sun, *Dalton Trans.*, **2015**, 44, 12282–12291; (c) S. Du, S. Kong, Q. Shi, J. Mao, C. Guo, J. Yi, T. Liang, W.-H. Sun, *Organometallics*, **2015**, 34, 582−590.
21. (a) S. Yuan, E. Yue, C. Wen, W.-H. Sun, *RSC Adv.*, **2016**, 6, 7431−7438; (b) Q. Xing, K.

Song, T. Liang, Q. Liu, W.-H. Sun, C. Redshaw, *Dalton Trans.*, **2014**, 43, 7830−7837.
22. (a) D. Gong, W. Liu, T. Chen, Z.-R. Chen, K.-W. Huang, *J. Mol. Catal. A: Chem.*, **2014**, 395, 100–107; (b) Z. Hao, B. Xu, W. Gao, Y. Han, G. Zeng, J. Zhang, G. Li, Y. Mu, *Organometallics*, **2015**, 34, 2783−2790.
23. W. Zhang, W.-H. Sun, S. Zhang, J. Hou, K. Wedeking, S. Schultz, R. Fröhlich, H. Song, *Organometallics*, **2006**, 25, 1961–1969.
24. (a) W. Zhang, W. Chai, W.-H. Sun, X. Hu, C. Redshaw, X. Hao, *Organometallics*, **2012**, 31, 5039–5048; (b) W.-H. Sun, S. Kong, W. Chai, T. Shiono, C. Redshaw, X. Hu, C. Guo, X. Hao, *Appl. Catal. A: Gen.*, **2012**, 447–448.
25. Y. Zhang, H. Suo, F. Huang, T. Liang, X. Hu, W.-H. Sun, *J. Polym. Sci., Part A: Polym. Chem.*, **2017**, 55, 830–842.
26. (a) S. Du, X. Wang, W. Zhang, Z. Flisak, Y. Sun, W.-H. Sun, *Polym. Chem.,* **2016**, 7, 4188–4197; (b) G. B. Galland, R. Quijada, R. Rolas, G. Bazan, Z. J. A. Komon, *Macromolecules,* **2002**, 35, 339−345; (c) W.-H. Sun, X. Tang, T. Gao, B. Wu, W. Zhang, H. Ma, *Organometallics,* **2004**, 23, 5037–5047.
27. (a) Y. He, X. Qiu, J. Klosin, R. Cong, G. R. Roof, D. Redwine, *Macromolecules*, **2014**, 47, 3782−3790; (b) V. Busico, R. Cipullo, N. Friederichs, H. Linssen, A. Segre, V. V. A. Castelli, G. V. D. Velden, *Macromolecules*, **2005**, 38, 6988−6996.
28. G. B. Galland, R. F. de Souza, R. S. Mauler, F. F. Nunes, *Macromolecules*, **1999**, 32, 1620–1625.

GRAPHICAL ABSTRACT

ZHENG WANG, YOUFU ZHANG, YANPING MA, XINQUAN HU,* GREGORY A. SOLAN,* YANG SUN, WEN-HUA SUN*

Molecular Weight Control of Polyethylene Waxes using a Constrained Imino-Cyclopenta[*b*]pyridyl-Nickel Catalyst

Nickel(II) bromide complexes bearing *N,N*-imino-cyclopenta[*b*]pyridines, upon activation with either MMAO or Et_2AlCl, exhibited high activity towards ethylene polymerization, producing polyethylenes with low molecular weights, narrow molecular weight distributions as well as unsaturated vinyl and vinylene functionalities.